DOI: 10.5281/zenodo.17359760

CHAPTER 19

Synthesis Techniques and Thermal Properties of Chalcogenide Glassy Alloys

Sunil Kumar

Department of Physics, Government Post Graduate College, Bisalpur, Pilibhit 262201 Uttar Pradesh, India

Corresponding author Email: skcbhu07@gmail.com

Received: 13 August 2025; Accepted: 13 October 2025; Available online: 15 October 2025

Abstract: Combining chalcogen elements usually selenium (Se), or tellurium (Te) sulfur (S), with other elements like tin (Sn), germanium (Ge), arsenic (As), indium (In) or antimony (Sb), produces chalcogenide glasses. The wide range of infrared transparency, nonlinear optical characteristics, and photonic uses of these glasses make them unique. These glasses can be prepared by using a number of techniques, including melt-quenching, vapour deposition and sol-gel but the melt-quenching approach is the most widely used. Analysis of various thermal parameters of chalcogenide glasses, including T_g (glass transition temperature) T_c (crystallization temperature), thermal stability parameter, Hruby Parameter, glass and crystallization activation energy for glassy and crystallization region, crystallization rate constant, enthalpy, etc by using DSC in non-isothermal conditions. Thermal transport properties of

Materials Science: Advances in Synthesis, Characterization and Applications (Vol. 1) - Digambar M. Sapkal, Harshal M. Bachhav, Gaurav Mahadev Lohar, Sanjay P. Khairnar (Eds.)

ISBN: 978-93-95369-55-8 (paperback) 978-93-95369-46-6 (electronic) | © 2025 Advent Publishing.

https://doi.org/10.5281/zenodo.17359760

chalcogenide glasses (CGs) thermal conductivity, thermal diffusivity and specific heat per unit volume are also observed by using transient plane source technique (TPS).

Keywords: Differential scanning calorimetric (DSC), Thermal stability, Transient Plane Source Technique (TPS), Activation energy Thermal Conductivity and Thermal Diffusivity

1. Introduction

Rapid cooling of melt to solidification prior to crystallization creates glassy solids. Although a glass has a random structure similar to that of a liquid, it has an extremely high viscosity (~10 ^{13}poise), which is almost the same as that of a solid (~$10^{14.6}$poise). Because of a certain temperature known as the glass transition temperature, glasses vary from other non-crystalline materials. Rapid cooling below this temperature turns a liquid into glass. The VI group elements (S, Se, and Te) of periodic table are used to make chalcogenide glasses. These glasses function as semiconducting substances. The potential uses of these glasses in optical devices and solid-state electronics including, photolithography, non-linear optics, optical imaging, memory switching, phase change optical recording, and, have sparked interest in them in recent years.[1–6] Digital X-ray imaging and TV pick-up tubes both use selenium-rich alloys. Long polymeric Sen chains are randomly combined to form amorphous Se with twofold coordination. Due to the size and the additional electrons in this orbit, Te causes modifications in interchain secondary bonds or Vander walls bonds when it is added to Se. The lower crystallization temperature, aging effect and lower thermal stability are characteristics the binary (CGs).[7, 8] The addition of third element in binary (CG) work as chemical modifier and improve the thermal, optical and physical properties of theses glasses.[9] As has been extensively explored in the literature, one method for examining crystallization kinetics is differential scanning calorimetry (DSC).[10,11] Both isothermal and non-isothermal experiments can be used to study thermal changes in the glassy alloys.[12,13] The heat evolved during the crystallization process is considered as a function of time in the isothermal system, which uses rapidly raising the sample's temperature above the T_g.

In the non-isothermal method, the sample is heated at a fixed rate and the heat that forms is again measured as a function of temperature or time. The inability to instantly attain a test temperature and the inability to take measurements while the system is stabilizing are drawbacks of the isothermal technique. This disadvantage does not apply to an experiment with a constant heating rate.[14] Finding the crystallization kinetics for a single alloy using several techniques is interesting.

Impurity additions such as Sn are especially interesting since they have significantly altered the thermal, optical, and electrical, characteristics of (CGs). The manufacturing of the device, which may be altered by adding the tin (Sn), is largely dependent on the material's optical gap and lattice perfection. The crystallization kinetics and thermal stability of Se–Te–Sn-In multi-component (CGs) was reported by Kumar and Singh.[15] Glass transition kinetics and thermal stability of $Se_{90-x}Te_5Sn_5In_x$ multi-component

ISBN: 978-93-95369-55-8 (paperback) 978-93-95369-46-6 (electronic)

(CGs) were reported by Singh and Kumar.[16] The synthesis methods and thermal characteristics of chalcogenide glasses are covered in this chapter.

2. Synthesis Techniques for Chalcogenide Glasses (CGs)

Although the melt quenching process is used to synthesis ChGs in bulk, thin film integration is necessary for the majority of ChG functional applications. According to the literature, there are a number of methods for creating chalcogenide glass in bulk and thin films. Certain devices, such as phase change memory devices, needed a thick, precisely thin film of a few nanometers to be deposited quickly and conformally coated.[17-20]

2.1. Melt Quenching Technique

The process of melt quenching is essential when creating glasses. The necessary amounts of the high purity (99.999%) components for the melt quenching procedure were weighed using an electronic scale. The high-purity materials with the necessary mixture ratio of elements were sealed into quartz ampoules (length 5 cm and inside diameter 8 mm) under a vacuum of 10-6 Torr to guarantee the homogeneity of the samples. The ampoules were then heated to the required temperature in a furnace at a rate of 3–4 K/min, and they were kept there for 8–10 hours. The molten samples were then quenched with ice-cooled water. The quenched sample has the shape of glasses. The amorphous nature has been demonstrated by the X-ray diffraction pattern.[16]

2.2. Thin Film Techniques

The literature has a number of thin film deposition methods that have been employed by various research communities. Based on their instrumentation and underlying physical and chemical principles of action, these approaches can be classified as either physical or chemical. Sublimation, evaporation, and ionic processes are examples of physical processes used in the physical vapor deposition (PVD) technology. When atoms are transferred from a solid or molten source onto a substrate, impingement is a crucial factor. These methods create thin films of elements, alloys, or compounds with thicknesses ranging from a few nanometers to micrometers. The two PVD processes that are most frequently employed are evaporation and sputtering.

2.2.1. Thermal Evaporation Technique

Using a molybdenum boat and vacuum evaporation, thin films of a sample were applied to clean glass substrates while maintaining base pressure and the substrate at ambient temperature. Following a soap solution wash, trichloroethylene ultrasonography, and an acetone dip, the glass substrates were cleaned. Following a final cleaning with double-distilled water, the substrates were dried in an oven set at roughly 100°C. A quartz- crystal analyzer was employed to control the evaporation rates and film thickness. The films' thickness is μm. The thin films were kept at the proper temperature inside the deposition chamber to attain thermodynamic equilibrium, as advised by Abkowitz[21] in chalcogenide glasses. In order to compare the results for various samples, the ambient conditions and deposition parameters were maintained

ISBN: 978-93-95369-55-8 (paperback) 978-93-95369-46-6 (electronic)

constant for each sample. A reference glass substrate was positioned in the path of one beam of a double beam spectrophotometer to measure the optical absorbance of films in the μm spectral band.

2.2.2. Flash Evaporation Technique

Using a modified feeder in a coating machine, thin films of the sample were created using the flash evaporation technique on ITO-coated glass substrates at room temperature in a vacuum chamber at pressures lower than 5×10-6 mbar. A molybdenum boat was used to evaporate a 99.99% pure sample powder that was provided by Standard Company. The powder was put in one of the disk's bins. In order to evaporate the sample powder, it was moved into a boat that had been heated to a temperature of roughly 1500K. 40 nm and 800 nm thick thin films were made. Using an ultrasonic bath, the substrates were washed in acetone and methanol before being dried with nitrogen gas.

Additionally, the substrates underwent glow discharge cleaning prior to sample deposition. About 15 centimeters separated the source from the substrate. The films were taken out of the coating chamber and let into the surrounding air after deposition.[22]

2.2.3. Sputtering Technique

Atom by atom or in clusters, the surface atoms are physically removed off a solid surface by the momentum transfer of gaseous ions accelerated from plasma to create high-quality thin films. The process of vaporization is not thermal. This process has a shorter source-to-substrate distance than the vacuum deposition method. To use this deposition method, an intensive ion bombardment of a sputtering target in a high vacuum setting using an ion gun or low-pressure plasma. With this method, the sputtered particle experiences infrequent or no gas phase contacts between the target and the substrate. Wenpeng Chen and A. van der Jagt A thin layer of $Tl_2SeAs_2Te_3$ chalcogenide glass was created using this method.[23] The earliest methods of sputtering are also magnetron, DC, and radio frequency sputtering.

2.2.4. Chemical Vapour Deposition Technique

This method involves transporting the gaseous chemical reactants to the reaction chamber (around the substrate) using thermally triggered or other means (such as plasma-assisted CVD or laser-induced CVD) so that the reaction can create a thin film on the substrate surface. Even on surfaces with complex forms, homogeneous films with low porosity can be deposited with this method. The main prerequisite for using this method to create thin films is a high vacuum. Numerous alternative techniques, such as the glow discharge method, spin coating technique, pulsed laser deposition technique, etc., can be used to create thin films from bulk materials.[24,25]

2.2.5. Glow Discharge Decomposition Technique

This method is based on the formation of plasma in a low-pressure gas, just like sputtering, but instead of ions from the plasma ejecting material from the target, the gas itself undergoes a chemical breakdown, which leads to the deposition of a thin film on a plasma-preserved substrate. The plasma is created by applying an r.f. field using either an inductive or capacitive connection. The film deposited with this

ISBN: 978-93-95369-55-8 (paperback) 978-93-95369-46-6 (electronic)

technique is significantly influenced by the gas pressure, flow rate, substrate temperature, and chamber geometry.[26]

2.2.6. Spin Coating Method

Curry and Mairaj[27] used the spin coating technique to create a thin layer of chalcogenide glass in 2005. The fluid's deposition onto the substrate and the subsequent removal of the coated substrate are the two processes that go into making an amorphous thin film. The film thickness can be increased by the same amount or decreased by an order of magnitude by changing the experimental conditions. The composition can be changed to change the viscosity of glass.[28]

2.2.7. Pulsed Laser Deposition Technique

Thin films were produced using pulsed laser deposition (PLD) on chalcogenide targets. Initially, bulk samples were made by synthesizing directly from pure components of evacuated silica ampoules.[29] Samples were then sliced and polished to produce parallel-faced PLD targets after this process. The thin films were deposited on static substrates at room temperature. Si substrates were cleaned with ethanol and acetone using ultrasonic vibration prior to being put in the deposition chamber. The films were deposited using a vacuum. The laser beam's angle of incidence was selected to provide constant target ablation.

Pulsed laser deposition (PLD) creates a plasma plume of the target material by ablation of the target's surface using a short laser radiation pulse. When the plume comes into contact with the substrate, its contents may cover it. Many studies have looked into the creation of thin films using pulse laser deposition technology. Numerous chalcogenide material types have been formed using this method.[30]

3. X-Ray Diffraction

The X-ray diffraction pattern reveals the presence of several phases within the substance. Crystalline materials exhibit significant crystalline peaks in patterns of X-ray diffraction due to the systematic arrangement of their atoms. The X-ray diffraction patterns found in amorphous or non-crystalline materials, however, exhibit a broad hump. This significant hump in the X-ray diffraction pattern of an amorphous solid is caused by random or uneven atomic distribution inside materials. (see Fig.1).

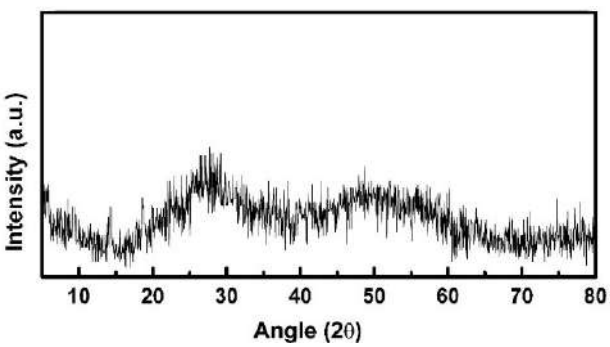

Fig. 1. XRD pattern of a particular chalcogenide glass

ISBN: 978-93-95369-55-8 (paperback) 978-93-95369-46-6 (electronic)

4. Thermal Properties

Differential Scanning Calorimetry (DSC)

Calorimetry was used to study the thermal properties of solids for over 100 years. It is still thought to be among the best methods for determining the kind of phase transitions that occur in glassy materials. Although calorimeters come in a wide variety nowadays, they can be broadly categorized into two groups. Devices in the first category measure the heat transfer between a sample and a thermal block while continuously adjusting the calorimeter's temperature. Most of them need a dummy sample (differential scanning calorimeter, DSC) in order to function differentially.The term "non-isothermal mode" describes these DSC observations. The calorimeters in the second group adiabatic, relaxation and ac calorimeters measure the sample's temperature when a very small quantity of heat is applied. The calorimeter's temperature is maintained during the measurement in these kinds of DSC equipment. First-order phase transitions are specifically investigated in DSC.

DSC curve of particular glassy alloys at heating rate 15 K/min is shown in Fig. 2. The first endothermic-like phenomenon indicates the glass transition region, which arises due to an abrupt increase in the specific heat of the sample. The second is the exothermic peak, which arises due to the crystallization process of the sample. Fig. 2 shows that the glass transition temperature (T_g) crystallization temperature (onset) T_c and crystallization temperature (peak)T_p and (T_c-T_g) thermal stability.

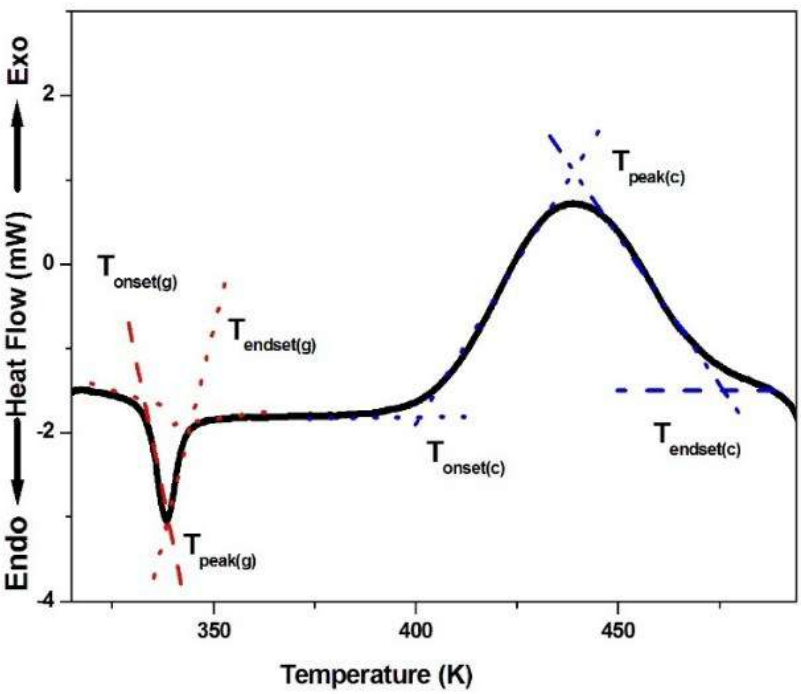

Fig. 2. DSC thermograms of the particular chalcogenide glasses at 15K/min heating rate.

ISBN: 978-93-95369-55-8 (paperback) 978-93-95369-46-6 (electronic)

Set-up description

Differential scanning calorimetry, or DSC, is a technique for calculating the energy needed to produce almost zero temperature differences between a substance and an inert reference material. Following exposure to the identical temperature regimes in a controlled-rate heated or cooled environment, the two specimens are displayed in Fig. 3. In this type of DSC, the sample and reference are connected by a low-resistance heat flow path. A single furnace covers the assembly. The sample's temperature differs from the reference due to changes in enthalpy or heat capacity. The observed temperature differential is connected to the enthalpy change.

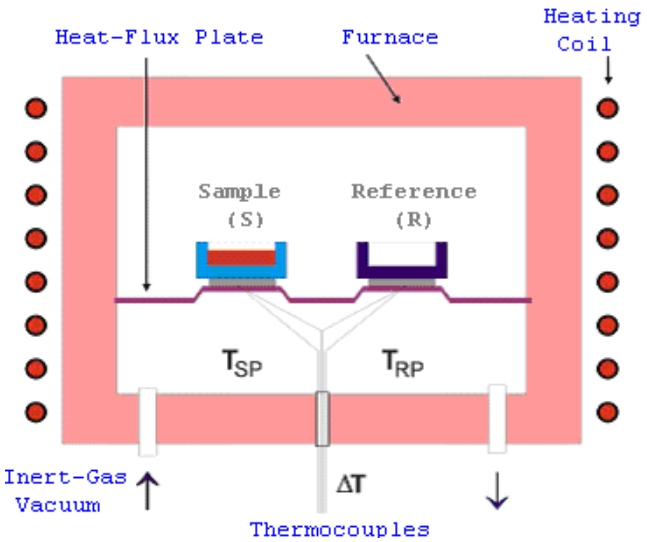

Fig. 3. A schematic framework *Heat flux DSC*

Working Principle of DSC

In heat flux DSC, the reference and sample pans are stored in the same furnace. The difference in heat required to maintain the reference and sample at a nearly equal temperature causes the sample to undergo thermal change because of excessive energy conduction between them though an attached metallic disc. Because the temperature differential that forms between the sample and the inert reference pans corresponds to the heat flow between them, the system's thermal resistances vary with temperature. This shift was recorded in calibrated mode, which automatically adjusts the amplification with temperature to offer a nearly constant calorimetric sensitivity. Because the sample material is not in close contact with the thermocouples, several temperature variations between the specimen and thermocouples occur during the operation. Consequently, the precise ΔT is not equal to $T_{S_0} - T_{R_0}$, where T_{R_0} and T_{S_0} are the temperatures of reference and sample respectively. The $T_{S_0} - T_{R_0}$ deduce from allowing for the heat flow paths in the system, as block diagram shown in Fig. 4.

ISBN: 978-93-95369-55-8 (paperback) 978-93-95369-46-6 (electronic)

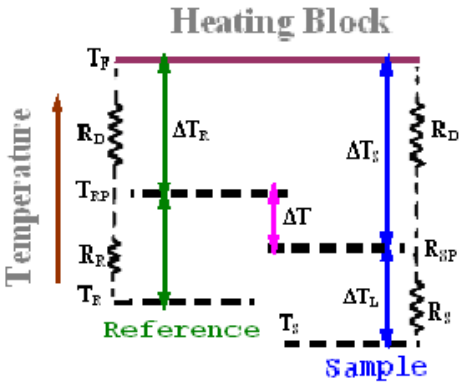

Fig. 4. A schematic framework of a Heating block of DSC

The used terminologies are defined as;

T_s, T_r = Temperature of the sample and reference platform in that order. T_{Sp} normally plotted as the abscissa of a DSC curve.

T_f = Temperature of the silver heating block.

R_d =Thermal resistance between the furnace wall and the sample or reference

Platforms (units Cmin J^{-1}).

R_{S_0}, R_{R_0} = Thermal resistances between the sample and reference platform.

C_{S_0}, C_{R_0} = Heat capacity of the sample and reference with particular containers.

H = Imposed heating rate.

ΔT_{R_0} = Temperature lags of the reference platform relative to furnace.

ΔT_{S_0} = Temperature lags of the sample platform comparative to furnace.

ΔT_{l_0} = Temperature lags of the sample comparative to the sample thermocouple.

$$\Delta T_{R_0} = HR_d C_{R_0} \quad (1)$$

$$\Delta T_{S_0} = HR_d C_{S_0} \quad (2)$$

$$\Delta T = HR_d \left(C_{S_0} - C_{R_0}\right) \quad (3)$$

ISBN: 978-93-95369-55-8 (paperback) 978-93-95369-46-6 (electronic)

$$\Delta T_{l_0} = HR_{S_0} C_{S_0} \quad (4)$$

$$\Delta T_{S_0} = \Delta T_{R_0} + \Delta T \quad (5)$$

$$\Delta T_{l_0} = \frac{R_{S_0}}{R_d \Delta T_{S_0}} \quad (6)$$

Temperature Calibration

Under the DSC furnace configuration, the temperature curve has been drawn on the abscissa of a DSC data that corresponds to the emf produced by the thermocouples. Using identified calibration tables, the emf can be accurately converted to temperature units for normal thermocouple conditions.

Calorimetric Calibration

Measurements of the sample's changes in specific heat or enthalpy are used to perform calorimetric calibration. Equation (2) can be used to define the change in specific heat in order to use the DSC device in calibrated mode. The heat flux DSC system's balancing heat equation is as follows:

$$\frac{dH'}{dt} = \frac{T_s - T_r}{R_d} + \left(C_{S_0} - C_{R_0}\right)H + C_{S_0}\left(\frac{R_d + R_{S_0}}{R_d}\right)d\left(\frac{T_s - T_r}{dt}\right) \quad (7)$$

$\frac{dH'}{dt}$ refers to the heat evolution of an exothermic transition; the first term on the right displays the area under the DSC peak with the baseline correction value. The second term on the right is the actual baseline that is utilized to determine specific heat. The third term, which is independent of the DSC peak area but could distort the peak form, explains that the specimen will use some of the evolved heat to heat itself. Equation (7) makes it evident that the second term can be utilized to calculate specific heat when the $\frac{dH'}{dt}$ value of is equal to zero. By comparing the thermal lag of the reference and sample DSC pans, the approach can be used. To do this, the system must first be calibrated using a standard specimen that comes with the equipment.

$$C = \frac{E_q Y}{H_0 M_0} \quad (8)$$

where M_0 is the mass of the sample, E is a calibration stable, C is the specific heat capacity of the standard sample, q is the Y -axis range and term Y is the variation in deflection between actual sample and standard sample. The enthalpy changes can be resolute by measuring the area under peak of the DSC curve. After all plot a relation ΔT against time, which verify the equation (1).

ISBN: 978-93-95369-55-8 (paperback) 978-93-95369-46-6 (electronic) | © 2025 Advent Publishing.

5. Thermal Conductivity and Thermal Diffusivity Measurements.

The structure, density, porosity, and other characteristics of a solid greatly influence its thermal conductivity and diffusivity, which vary depending on the substance, because of the wide range of thermal transport characteristics; these physical parameters are highly dependent on temperature and pressure. Applications such as space shuttles, biomaterials, and the thermal control of electronic packages in semiconductor industries depend on a material's thermal diffusivity and thermal conductivity.

6. Transient Plane Source Techniques (TPS)

Because hot disk transient plane source techniques assess thermal conductivity and thermal diffusivity of materials quickly and accurately, they have become quite popular in recent years. Gustafsson invented this method in 1967.[31] Although this instrument sensor was initially intended to be rectangular in shape (as a hot strip sensor), it is theoretically possible for it to take on any shape. A wide spectrum of material transport qualities have been covered by the TPS approach. The Hot Disk is a device that measures the specific heat per unit area, thermal diffusivity and thermal conductivity of solid and fluid materials in the temperature range of 30 K to 1000 K without causing any damage. Metal, alloys, ceramics, minerals, polymers, composites, glass, textiles, paper, glass, wool, foam, powders, and biomaterials can all have their thermal conductivity and thermal diffusivity measured using this device. It can also be used to determine the thermal properties of anisotropic materials.

It is essential for the design of any TPS element that the pattern cover the electrically conducting pattern and occupy as much of the "hot" area as feasible, provided that there is insulation between the pattern's various components. This is especially critical when the samples' surfaces and conduction pattern are covered with insulating layers. It should be mentioned that beyond a brief initial transient, the temperature differential across the insulating layers is assumed as constant.

Set-up description

With an insulating layer of 50 μm thick Kapton on each side of the metal outline, the TPS element is collected of 10 μm (Fig. 5a) thick nickel foil (with a resistance of around 3.26 Ω and a TCR 4.6×10^{-3} K^{-1}). Fig.5b and 5c, respectively, depict the sample holder and the electrical circuit schematic diagram used to evaluate thermal conductivity and thermal diffusivity.

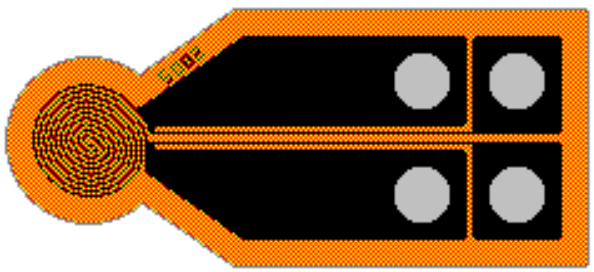

Fig. 5a. Schematic framework diagram of TPS sensor

ISBN: 978-93-95369-55-8 (paperback) 978-93-95369-46-6 (electronic)

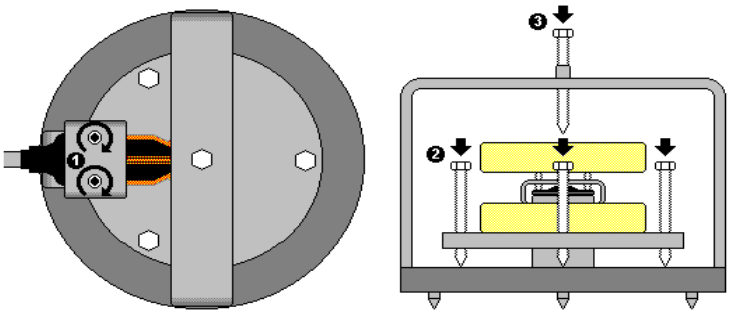

Fig. 5b. Schematic framework Sample holder diagram with TPS sensor.

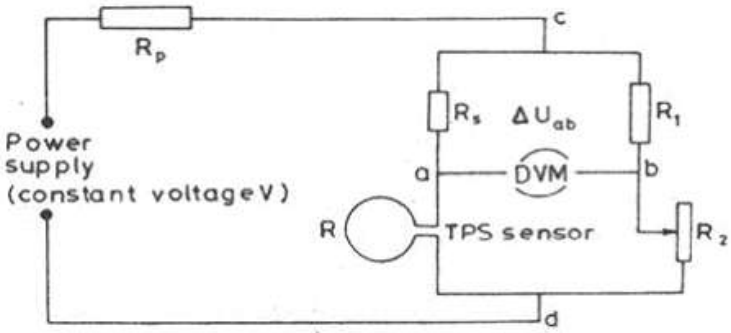

Fig. 5c. Schematic framework diagram of the electrical circuit for measurement of thermal conductivity and thermal diffusivity

Working Principle

In the same manner as described by Gustafsson, evaluations can be carried out using experimental data from TPS measurements.[32,33] During a transient recording, these device measures values of thermal conductivity, thermal diffusivity, and specific heat per unit volume. A certain time window should be chosen for the entire recording in order to collect the aforementioned physical quantities, and their characteristics should be calculated by dividing the square of the sensor's radius by the diffusivity material under test. The TPS instrument's software automatically delivers the required indication, ensuring that the display criteria are met and that the experiment was carried out successfully. The operator can use this software signal to validate that the results are reliable. The voltage measured during the first few seconds of tests with such substantial insulating layers must be disregarded due to the influence of the insulating layers. However, the characteristic time of the experiment is so long due to the enormous heated surface of the TPS element that a few seconds of the acquired potential difference values can be ignored. Despite this, the outcomes are outstanding. To ensure the accuracy of these results, the experiment is conducted and recorded at room temperature or the required temperature on multiple occasions. Additionally, the samples (pellets measuring 12 mm by 2 mm) must be kept at room temperature or at the desired temperature for at least two hours prior to the collection of experimental data in order to achieve thermal

ISBN: 978-93-95369-55-8 (paperback) 978-93-95369-46-6 (electronic)

equilibrium. A digital voltmeter has been used to record the voltage variations. The output power can be varied based on the type of spaceman material and typically falls between 6×10^{-6} and 16×10^{-6} W/m^2 of the sample.

7. Conclusions

This chapter discusses the synthesis methods and thermal characteristics of chalcogenide glasses. In order to manufacture these glasses, I have covered bulk glassy and thin film synthesis procedures. In order to be coated rapidly and conformably, some devices, including phase change memory devices, required a thick, perfectly thin film of a few nanometers. DSC has been used to assess T_g, T_c, T_m, specific heat, thermal parameters, etc. under non-isothermal circumstances. Thermal transport properties were all effectively assessed using the Transient Plane Source technique (TPS).

Acknowledgements

We wish to express our thanks to Department of Physics Institute of Science, B.H.U. Varanasi, for undertaking the XRD measurements. For the financial support under the Research & Development Scheme, I am grateful to Higher Education, Uttar Pradesh.

References

1. T. Katsuyama, S. Satoh, H.M. Atsumura, optical fibre, J Appl. Phys., 1992, 71, 4132–6.
2. S.R. Elliot, Physics of amorphous materials, 2nd ed. London Longman, 1991.
3. M. Asobe, Opt Fiber Technol. 1997; 3:142–8.
4. M. Frumar, Z. Cernosek, J. Jedelsky, B. Frumarova, T. Wagner, J Optoelectron Adv Mater., 2001;3, 177–88.
5. T. Wagner, M. Frumar, V. Suskova, J Non-Cryst. Solids. 1991; 128:197–207.
6. K. Ramesh, S. Asokan, K.S. Sangunni, E.S.R Gopal, J Phys Chem Solids., 2000, 61, 95.
7. A.K. Vashneya, D.J. Mauro, J Non-Cryst. Solids., 2007, 353, 1291–7.
8. M.N. Kozicky, M. Mitkova, J Non-Cryst Solids.2006; 352:567–77.
9. A. K. Singh, N. Mehta, K. Singh, Eur J Appl Phys. 2009, 46, 20303.
10. A.A. Elabbar, M. Abu El-Oyoun, A.A. Abu-Sehly and S.N. Alamri, J. Phys. Chem. Solids 2008, 692, 527.
11. A.A. Joraid, A.A. Abu-Sehly, M. Abu El-Oyoun and S.N. Alamri, Thermochim. Acta, 2008, 470, 98.
12. N. Rysava, T. Spasov and L. Tichy, J. Therm. Anal, 1987, 32 p.1015.

ISBN: 978-93-95369-55-8 (paperback) 978-93-95369-46-6 (electronic)

13. N. Afify, J. Non-Cryst. Solids, 1991, 128, 279.
14. M. J. Strink, A.M. Zahra, Thermochim. Acta, 1997, 298 p.179.
15. S. Kumar, K. Singh, Physica B, Physica B 406 (2011) 1519–1524
16. S. Kumar, K. Singh, Thermochimica Acta, 2012, 528, 32– 37.
17. M. Birkholz P. F. Fewster, and C. Genzel, Thin Film Analysis by X-Ray Scattering. Weinheim: Wiley-VCH, 2005.
18. M. Ohring, Materials Science of Thin Films (2nd ed.). Boston: Academic Press, 2001.
19. K. Seshan, Handbook of Thin Film Deposition (3rd ed.). Amsterdam: Elsevier, 2012.
20. K. L. Chopra, Thin Film Phenomena. N. Y.: McGraw-Hill Book Company, (1969).
21. M. Abkowitz, Polym. Engg. Sci. 1984.24, 1149
22. M. H. EHSANI, H. REZAGHOLIPOUR DIZAJI, Chalcogenide Letters 2011, 8, 33.
23. A. van der Jagt Chen. Wenpeng, J. Vac. Sci. Technol. A, Vol. 4, No. 2, Mar/Apr 1986.
24. M. Lazell, P. O'Brien, D. J. Otway, J. Park, J. Chem. Soc., Dalton Trans. 2000, 24, 4479.
25. J. Etzkorn, H. A. Therese, F. Rocker, N. Zink, U. Kolb, W. Tremel, Adv. Mater., 2005, 17, 2372.
26. D. R. Reyes, M. M. Ghanem, G. M. Whitesides, and A. Manz, Lab on a Chip. ACS. 2002, 2, 113.
27. R. J. Curry, A. K. Mairaj, C. C. Huang, R. W. Eason, C. Grivas, D. W. Hewak, and J. V. Badding, J. Am. Ceram. Soc., 2005. 88, 2451.
28. D. W. Harwood, E. Taylor, R. Moore, D. N. Payne, J. Non-Cryst. Solids, 2003.332, 190.
29. M. Essi, N. Kouame, G. Cisse. Chalcogen. Lett., 2018, 15, 379.
30. A. K. Mairaj, R. J. Curry, D. W. Hewak, Electron. Lett., 2004, 40, 412–22.
31. S.E., Gustafsson, Rev. Sci. Instrum, 1991, 62, 797.
32. Yi. He, Thermochimica acta, 2005, 436, 122.
33. M. Gustavsson, S. E. Gustafsson, 2006, 442, 1.

ISBN: 978-93-95369-55-8 (paperback) 978-93-95369-46-6 (electronic)